Journal of Animal Science, 2023, **101**, 1–11
https://doi.org/10.1093/jas/skac373
Advance access publication 13 November 2022
Economics of Animal Production

Nonlinear model fitting analysis of feather growth and development curves in the embryonic stages of Jilin white geese (*Anser cygnoides*)

Yudong Wang, Xianou Fu, Sihui Wang, Ichraf Mabrouk, Yuxuan Zhou, Yupu Song, Tuoya Liu, Jingyun Ma, Fangming Zhuang, Xue Zhang, Keyi Xu, and Yongfeng Sun[1]

Key Laboratory of Animal Production, Product Quality and Security, Jilin Agricultural University, Ministry of Education, Changchun 130118, China

[1]Corresponding author: sunyongfeng@jlau.edu.cn

Abstract

Poultry is subject to varying degrees of feather loss and feather pecking during production, which seriously affects the live appearance and carcass appearance of their commercial traits and greatly reduces the production profitability of the farming enterprise. It also has an impact on down production and quality in the case of geese. In this study, mathematical models (Logistic, Gompertz, and Von Bertalanffy) were used to assess feather growth and development during the embryonic period in Jilin white geese (*Anser cygnoides*) predicting the weight and length of feathers from the back, chest, and belly tracts at different embryonic ages, to determine which growth model more accurately described feather growth patterns. The result first showed that the primary feather follicles of the Jilin white goose developed at E14 and secondary feather follicles at E18; primary feather follicle density increased and then decreased, whereas secondary feather follicle density increased continuously and the primary and secondary feather follicles developed independently. Secondly, the embryonic feather growth followed a slow–fast–slow pattern, with feathers growing slowly from E12 to E18, quickly from E18 to E24, and then decreasing after E24 until just before emergence (E30). In addition, before E14, feathers were concentrated in the back tracts, and no feathers were found on the head, neck, chest, abdomen, or wings. By E22, the whole body of the embryo was covered with feathers, and the back feathers were the earliest and fastest to develop. Compared to the Gompertz and von Bertalanffy models, the logistic model fit (R^2 = 0.997) was the highest, while the sum of residual squares (RSS = 25661.67), Akaike's information criterion (AIC = 77.600), Bayesian information criterion (BIC = 78.191), and mean square error (MSE = 2851.296) were the lowest. Therefore, the logistic model was more suitable for describing the changes in whole-body feather growth during the embryonic period in Jilin white geese. In conclusion, using the growth curve model to explain the relationship between feather growth and embryonic age in geese will potentially speed up the process of genetic improvement in Jilin white geese (*A. cygnoides*) and thus provide scientific support for molecular genetic breeding.

Lay Summary

Feathers are an important external feature of poultry, and feather follicles are important appendages to the skin. Especially for geese, feather follicle development largely determines feather length and quality, which in turn affects feather-related economic traits. The growth curve is to use mathematical equations to fit the growth and development curve and analyze the growth and development laws of livestock and poultry. Therefore, whether the establishment of a growth curve model can be used to describe the growth process between the embryonic feather weight, length, and embryo age of the Jilin white goose will be worth further study.

Key words: feather follicles, feather mass, feather length, growth curve, Jilin white goose

Abbreviations: AIC, Akaike's information criterion; BIC, Bayesian information criterion; E, Embryonic age; MSE, mean square error; RSS, residual sum of squares; R^2, R-squared

Introduction

As we all know, goose down, goose liver andgoose oil are highly valuable raw materials for textiles, food, and chemicals, and goose down as a light and warm textile material that has been widely used in people's daily lives (Kozak et al., 2010). The survey found that geese in the large-scale breeding process experience different degrees of feather loss and pecking phenomena, which not only affect the down production and quality but also affect the commercial traits of geese in the live appearance and carcass appearance, greatly reducing the production profit of breeding enterprises. In addition, as people's traditional eating habits and cooking methods change, chilled geese are gradually replacing live birds and becoming the main purchase object for consumers, while the size of the chilled goose feather sac is an important carcass trait that directly affects consumers' desire to buy (Boz et al., 2019). Feather follicle is the site of feather production and growth in poultry and controls the rate of feather growth, down quality and feather regrowth (HU et al., 2020). For this reason, more and more breeders are paying attention to the growth and development patterns of the skin follicles in geese.

Received September 23, 2022 Accepted November 10, 2022.

The Jilin White Goose is one of the main breeds of goose circulating in Jilin Province, China. The adult goose has white feathers with good fluffiness and an average down content of up to 30%. Feathers are keratinized derivatives of the skin that cover the surface of the carcass, starting from the feather follicles and developing from the ectodermal cells during embryonic life, and are used to maintain flight and regulate body temperature (Kondo et al., 2018). Depending on the external morphology and distribution of the feathers, there are two main types of feathers: orthodermal feathers, which develop from primary feather follicles, and downy feathers, which develop from secondary feather follicles (Chen et al., 2015; Zou et al., 2020). Feather follicles are microscopic structures that are part of the cyclical cycle of the skin and are generally divided into anagen, regression, and resting phases (Chen et al., 2016). During the development of goose follicles, primary and secondary follicles develop independently and the primary follicles develop slightly earlier than the secondary follicles, and both show a cyclical cycle of follicular regeneration (Wu et al., 2008). It can be seen that the production of feathers is highly correlated with the development of feather follicles.

Growth and development are continuous biological processes. Growth refers to the growth of organ systems and overall body size and development refers to the refinement of cell differentiation and functional maturation. Therefore, growth and development are fundamental characteristics of living organisms (Tompic et al., 2011). In contrast, growth curves are used to dynamically describe and analyze the growth and development patterns of livestock and poultry to fit growth and development curves with mathematical equations to describe the process of weight gain over time or age and to understand the interrelationships between model parameters and biological characteristics (Ricklefs et al., 1985). Currently, the nonlinear fitting models that have been applied in poultry are the Logistic, Gompertz, and Von Bertalanffy models, such as for chickens, ducks, and pigeons (Aggrey et al., 2002; Vitezica et al., 2010; Gao et al., 2016). Although there is a high correlation between the length of feathers at different plumage zones in poultry, studies of feather growth by curve fitting have rarely been reported.

Therefore, this study used mathematical models (Logistic, Gompertz, and Von Bertalanffy) to assess the embryonic feather growth and development of the Jilin White Goose and to predict the weight and length of back, belly, and chest feathers at different embryonic ages. The aim was to fit the embryonic feather growth and development curves of Jilin white geese (*Anser cygnoides*) using three nonlinear functions and then to derive the most suitable embryonic feather growth curve for Jilin white geese to provide a theoretical basis for genetic improvement of Jilin white geese.

Materials and Methods

Ethical statement

Goose embryos were executed using the cervical dislocation method. All animal experiments were performed following the relevant guidelines established by the China Animal Committee. All animal experimental procedures were approved by Jilin Agricultural University (approval number: GR(J)18-006), Date: 29 March 2018).

Experimental design and treatment

In this experiment, the required Jilin white goose fertilized breeder eggs (130 ± 5 g) were provided by Hongming Goose Industry in Yongji County, Jilin Province. The eggs were fumigated, weighed, labeled, and incubated in an incubator (Dezhou, Shandong, China) at a relative humidity and temperature of 60% and 37.8 °C (Guo et al., 2021), respectively. The eggs were turned over at a uniform rate for an average of 180 s every 2 h until embryonic day 30. At E7 of incubation, unfertilized and early embryonic death eggs were removed using an egg illuminator and the remaining eggs were incubated until a specific time point.

Sample collection and measurements

According to the group's previous experiments, the embryos were initially formed at E7 of incubation, and the feather buds were visible to the naked eye on the back skin of the goose embryos. Therefore, E12, E14, E16, E18, E20, E22, E24, E26, E28, and E30 were selected as the time points for sample collection. At each time point, 20 eggs were randomly selected, the blunt end of the egg shell was cracked with forceps, the egg contents were slowly poured into sterilized trays, the embryos were peeled with forceps and the state of the skin feather buds was physically observed with a body microscope. In addition, a portion of the goose embryo was sampled at the back, belly, and chest positions and placed in a 4% paraformaldehyde solution for 24 h to fix the tissue for sectioning and hematoxylin and eosin (H&E) staining. The other part of the goose embryo was used to collect the back, belly, and chest feathers, the back is the area behind the clavicle and above the wings, the chest is the area below the clavicle and above the trochanter, and the abdomen is the middle area below the trochanter and above the line of the sciatic and patellar bones. The collected feathers were dried in an oven at 65 °C for 24 h and weighed on an electronic balance (accuracy 0.0001 g). Finally, 100 feathers were randomly selected from the dorsum, abdomen and chest at each time point and the feather length, which is the distance from the root to the tip of the feather, was measured using an electronic vernier caliper (accuracy 0.01 mm) To ensure the sterility of the sampling process, the instruments used in the process were autoclaved ahead of time.

Histological observations

The tissue samples were removed from the 4% paraformaldehyde solution and placed in a labeled embedding cassette, then washed with tap water for 24 h. The samples were processed in the following order: 70% ethanol for 12 h, 80% ethanol for 12 h, 95% ethanol for 1 h, 100% ethanol twice for 1 h each, and xylene twice for 10 min. The samples were subsequently embedded in a KD-BM tissue embedding processor (Zhejiang Jihuaji Instruments Co., Ltd.) after 2 h of wax immersion and embedding. Tissues were cut into continuous longitudinal and transverse sections of the skin using a Leica RM2135 slicer (Leica Microsystems, Wetzlar, Germany) with a section thickness of 5 μm (Liu et al., 2018). Paraffin sections were dewaxed, hydrated, and stained with hematoxylin and eosin (H&E). All sections were observed under a Nicon-300 light microscope (Nicon, Tokyo, Japan) for back skin tissue feather follicle morphology and then photographed with different magnifications of the objective. Feather follicle density measurements were performed by selecting 10 consecutive

transverse sections (1 mm × 1 mm) of the same transverse skin area to count the number of feather follicles and then averaging them.

Growth modeling and assessment

An ideal growth curve model can not only infer the dynamic changes in poultry growth and development and guide the daily feeding management of poultry but also effectively eliminate the influence of some experimental errors. In order to obtain the most suitable model to describe the embryonic feather growth curve of the Jilin white goose, three different nonlinear functional growth models (Logistic, Gompertz, and Von Bertalanffy) were fitted to the length of the back, belly, and chest feathers at different embryonic ages, and the corresponding expressions and related parameters are shown in Table 1. Currently, these models have been proven to describe the growth and development of feathers in yellow-finned broiler chickens at embryonic and post-embryonic stages (Xie et al., 2020b).

Statistical analysis

Excel was used to build the database and the data were tested using one-way ANOVA, with the resulting values expressed as mean ± standard error. 1stOpt programming and SPSS 20.0 software were used to calculate the A, B, and k best estimates to build the growth models. Then, the inflection points embryonic age, inflection point feather mass or length, maximum daily gain, relative growth rate and absolute growth rate were calculated for each model, respectively. The models were assessed for merit based on goodness of fit (R^2), the chi-squared information criterion (AIC), the Bayesian information criterion (BIC), mean squared error (MSE), and t-test, and the model with the lowest AIC, BIC, and MSE was selected as the most appropriate model (Narinc et al., 2013; Nguyen et al., 2021). In which k is the number of parameters in the fitted model; n is the number of samples; RSS is the sum of squared residuals; and $\hat{Y}$ is the predicted value. Finally, GraphPad Prism 8 was used to plot the growth and development curves.

$$\mathrm{AIC} = n \times \ln\left(\frac{\mathrm{RSS}}{n}\right) + 2k$$

$$\mathrm{BIC} = n \times \ln\left(\frac{\mathrm{RSS}}{n}\right) + k\ln(n)$$

$$\mathrm{MSE} = \frac{\sum_{i=1}^{n}\left(Y_i - \hat{Y}_i\right)^2}{n-2}$$

Table 1. Jilin white goose embryonic feather Logistic, Gompertz, and Von Bertalanffy models and corresponding characteristic parameters

Growth model	Expressions[1]	Inflection day	Inflection feather mass or length	Maximum day growth value
Logistic	$Y = A/(1 + Be^{-kt})$	$(\ln B)/k$	$A/2$	$kw/2$
Gompertz	$Y = Ae^{-B\exp(-kt)}$	$(\ln B)/k$	A/e	kw
Von Bertalanffy	$Y = A(1 - Be^{-kt})^3$	$(\ln 3B)/k$	$8A/27$	$3kw/2$

[1]Y is the weight or length of the goose embryo feather observed at embryonic age t; A is the maximum feather mass or length; k is the instantaneous growth rate; B is a parameter; t is the corresponding embryonic age; w is the inflection point feather mass or length; e is a natural constant; and exp is a mathematical symbol.

Results

Feather follicles formation process in the embryonic stage of Jilin white goose

Feather growth and development during embryonic development of the Jilin White Goose are shown in Figure 1. At E12 of incubation, the back surface of the embryo is smooth and the skin is covered with a transparent layer of membranous material (Mabrouk et al., 2022). At embryonic stage E14, the skin of the goose embryo appears evenly and neatly elevated, the buds begin to grow from proximal to distal and the epidermis becomes somewhat invaginated, which is the prototype of the primary feather follicle (Figure 1B). At embryonic stage E16, the back, chest and abdomen of the gosling are covered with feathers (Figure 1A), and the skin surface is covered with bumps of varying sizes after plucking. At embryonic stage E18, the epidermis of the gosling is invaginated into the dermis and wrapped around the feather buds, marking the appearance of secondary feather follicles on the skin of the gosling (Figure 1B). From E18 to E30, the follicles mature and blood vessels, glands, and collagen fibers appear in the connective tissue surrounding the follicles. The present results indicate that secondary follicles form approximately 4 d later than primary follicles and it is assumed that primary and secondary follicles develop from the same feather primordium and that they both develop independently.

Microstructure of feather follicles

The microscopic images in Figure 2A–F showed the microstructure of the skin and feather follicles of Jilin white geese (*A. cygnoides*) at different embryonic ages. The results showed that at E14, the primary feather follicles presented an undifferentiated cylindrical outer epidermal wall, including the cuticle, middle layer, and basal layer (Figure 2A). In a micrograph of a cross-section of skin tissue at E16, multiple plumule ridges are clearly visible and undifferentiated plumule ridges are present near the root (Figure 2B). At E18, there are approximately 10 to 20 feather ridges, and a large number of blood vessels begin to appear in the central zone of the pulp (Figure 2C), and during secondary follicle formation, the feather ridges in the goose embryo follicles begin to differentiate into marginal plates, feather branchlet plates, and feather axial plates. As the feather follicles develop further, new barbed tracks begin to form and the boundary lines of the feather ridge become indistinguishable (Figure 2D). Later in embryonic development, the feather follicles gradually become completely filled with feather buds and feather follicle cavity disappears. At E24, the mature feather follicles are surrounded by muscles, nerves, glands, and a large number of blood vessels, presenting a quadrilateral arrangement of muscular networks in the dermis (Figure 2E). From E26 to E30, the structure of the feather follicle resembles the shape shown in Figure 2F, with a large number of dermal papilla cells clustered at the root of the follicle (Martel et al., 2022).

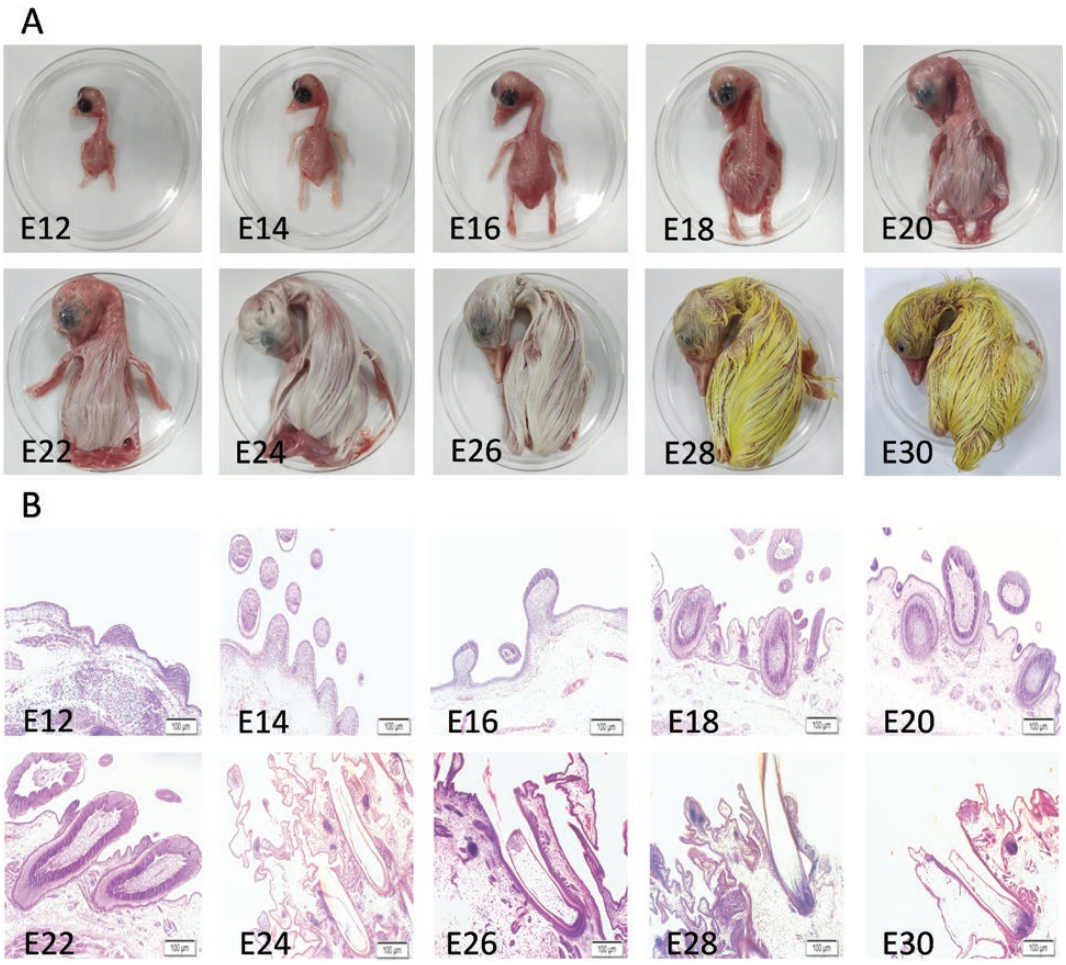

Figure 1. Feather growth and development during embryonic development in the Jilin white goose. (A) Observations on the external morphology of the embryonic feathers of the goose. (B) Microscopic observation of the skin follicles of the goose embryo at different stages of development by HE. Magnified: 100×; Bar: 100 μm.

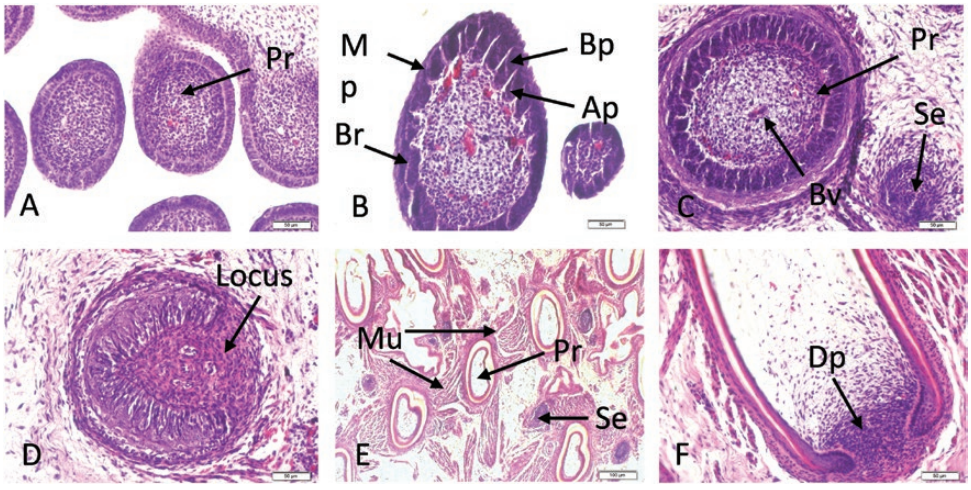

Figure 2. Microscopic observations of feather follicles at different stages of development in goose embryos. (A) Undeveloped barbed ridge (Br) in the back primary feather follicle (Pr) at embryonic day 14 (200×). (B) Transverse section of a feather follicle in E16 (200×), the skin showing Br that have been differentiated into three longitudinal plates: the marginal plate (Mp), the barbule plate (Bp), and the plumule axis plate (Ap). (C) Primordial period of secondary feather follicles at embryonic day 18 (200×). (D) Shows the formation of the new barb locus forming on the back skin at E20 (200×). (E) The fully developed feather muscles (Mu) on the back skin at E24 (100×). (F) The feather follicle root contains a large number of dermal papilla cells.

Table 2. Variation in the density of feather follicles in the back, chest, and belly feathers of goose embryos[1]

E	Back			Chest			Belly		
	Pr	Se	S/P	Pr	Se	S/P	Pr	Se	S/P
14	4.10 ± 0.2^{e}	–	–	3.85 ± 0.26^{e}	–	–	3.75 ± 0.32^{e}	–	–
16	6.85 ± 0.26^{d}	–	–	6.75 ± 0.43^{d}	–	–	6.95 ± 0.15^{d}	–	–
18	10.95 ± 0.61^{a}	1.95 ± 0.26^{e}	0.21	10.25 ± 0.55^{a}	2.15 ± 0.18^{d}	0.21	10.75 ± 0.55^{a}	1.15 ± 0.09^{d}	0.11
20	10.35 ± 0.26^{ab}	4.29 ± 0.17^{d}	0.40	9.95 ± 0.26^{ab}	3.95 ± 0.26^{c}	0.40	10.55 ± 0.72^{ab}	4.18 ± 0.27^{c}	0.40
22	10.25 ± 0.44^{ab}	4.95 ± 0.38^{d}	0.56	9.50 ± 0.38^{abc}	5.35 ± 0.38^{c}	0.56	9.85 ± 0.63^{abc}	4.95 ± 0.44^{c}	0.50
24	9.75 ± 0.49^{bc}	6.95 ± 0.49^{c}	1.06	9.37 ± 0.15^{abc}	9.95 ± 0.55^{b}	1.06	9.55 ± 0.43^{abc}	8.75 ± 0.67^{b}	0.92
26	9.24 ± 0.20^{bc}	9.15 ± 0.38^{b}	1.25	9.1 5 ± 0.15^{bc}	11.45 ± 0.83^{ab}	1.25	9.15 ± 0.26^{bc}	11.35 ± 0.73^{a}	1.24
28	8.95 ± 0.20^{c}	10.25 ± 0.64^{ab}	1.33	8.75 ± 0.26^{c}	11.65 ± 1.07^{ab}	1.33	8.75 ± 0.49^{c}	11.65 ± 0.89^{a}	1.33
30	8.75 ± 0.32^{c}	11.25 ± 0.78^{a}	1.40	8.55 ± 0.26^{c}	11.95 ± 0.90^{a}	1.40	8.72 ± 0.37^{c}	11.95 ± 0.95^{a}	1.37

Values are expressed as mean ± standard error (Mean ± SE); values in the same column labeled indicate differences in follicle density between germinal ages of the same follicle type ($P < 0.05$, $n = 3$).
Abbreviations: E, embryonic age; Pr, primary feather follicle; Se, secondary feather follicle.
[1]Pr indicates the density of primary feather follicles (follicles/mm^2); Se indicates the density of secondary feather follicles (follicles/mm^2); S/P indicates the ratio of secondary to primary follicles; "–" indicates no detected values.

Variation of feather follicles density in goose embryos

As seen in Table 2, the density of back primary follicles increased significantly from 4.01/mm^2 in E14 to 10.95/mm^2 in E18 ($P < 0.05$), the density of chest primary follicles increased significantly from 3.85/ mm^2 in E14 to 10.25/mm^2 in E18 ($P < 0.05$) and the density of belly primary follicles increased significantly from 3.75/mm^2 in E14 to 10.75/mm^2 in E18 ($P < 0.05$). Secondary feather follicles started to form at E18, the ratio of secondary to primary feather follicle density on the back increased from 0.18 in E18 to 1.29 in E30, the ratio of secondary to primary feather follicle density on the chest increased from 0.21 in E18 to 1.40 in E30 and the ratio of secondary to primary feather follicle density on the abdomen increased from 0.11 in E18 to 1.37 in E30. The results showed that the density of primary feather follicles on the back, chest, and belly parts of the goose embryo decreased and the density of secondary feather follicles increased with the increase in the surface area of the embryo, and the growth and development pattern of the feather follicles on the chest and belly parts remained basically the same.

Developmental patterns of whole-body feather growth in goose embryos and model fitting analysis

As shown in Figure 3 and Table 3, the whole-body feather mass of Jilin white goose embryos increased with embryonic age. At E14, when the eggs were hatched, the goose embryos began to grow feathers. Before E18, the whole-body feather mass showed a trend of slow increase. Between E18 and E24, the whole-body feather growth rate accelerated and at E21.5 d, the increment reached its maximum. From E24 to E30, the whole-body feather mass growth rate was slow. At E14, the whole-body feather mass was 26.4 ± 0.5 mg/goose and at E30, the total feather mass of goose embryos was 2280.3 ± 1.3 mg/goose, an increase of approximately 86.36 times compared to E14.

As shown in Table 4, the curve parameters of the three growth models, Gompertz, Logistic, and von Bertalanffy, were used to calculate the individual parameters and goodness of fit criteria for the feather growth inflection point.

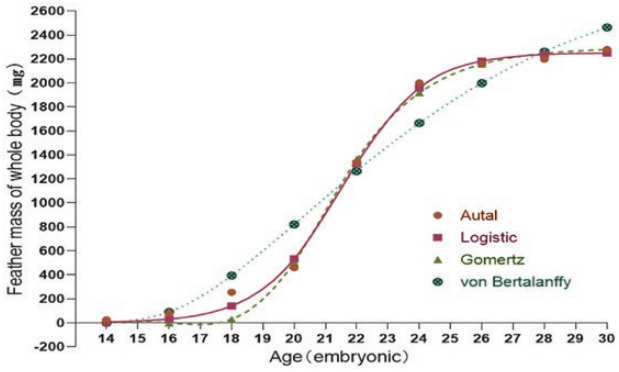

Figure 3. Actual measurements of whole-body feather mass in Jilin white geese (*Anser cygnoides*) at the embryonic stages, which were fitted to predicted values from three growth models: Logistic, Gompertz, and Von Bertalanffy.

The results showed that the logistic model can be used as the best-fit growth curve to describe the changes in whole-body feather mass during the embryonic period of the Jilin white goose. The inflection points for whole-body feather growth were at E21.5, 1126.6 mg, and 433.7 mg, respectively, with a goodness of fit (R^2) of 0.997 and a residual sum of squares (RSS) of 25661.67. Compared with the logistic model, the Gompertz and von Bertalanffy models were not as suitable for describing changes in whole-body feather growth during the embryonic period in Jilin white geese, with relatively low R^2 values of fit ($R^2_{\text{Gompertz}} = 0.991$, $R^2_{\text{von Bertalanffy}} = 0.971$) and relatively large RSS values of residual sum of squares ($RSS_{\text{Gompertz}} = 70389.05$, $RSS_{\text{von Bertalanffy}} = 229264.26$), and as shown in Figure 3, the predicted values from the logistic model can be found to be closer to the measured values of the whole-body feather mass of the goose embryos.

Variation pattern of goose embryo back feather mass and model fitting analysis

From Table 3, it can be seen that the back feathers of the Jilin white goose embryonic stage start to appear at E14, and the feather mass grows slowly at E14 to E18 stage. At the rapid growth stage, E18 to E24 stage, the feather mass grows fastest

Table 3. Patterns of change in goose embryo feather mass and feather length

E	Feather mass (mg)				Feather length (mm)		
	Whole body	Back	Chest	Belly	Back	Chest	Belly
14	26.4 ± 0.5^{i}	8.4 ± 0.3^{i}	0.9 ± 0.1^{i}	0.8 ± 0.1^{i}	4.94 ± 0.01^{i}	0.87 ± 0.01^{g}	0.68 ± 0.01^{g}
16	79.3 ± 0.6^{h}	23.5 ± 0.1^{h}	4.1 ± 0.3^{h}	3.5 ± 0.1^{h}	7.85 ± 0.03^{h}	2.11 ± 0.01^{f}	2.53 ± 0.01^{f}
18	254.9 ± 0.8^{g}	61.4 ± 0.5^{g}	18.5 ± 0.2^{g}	17.3 ± 0.2^{g}	10.84 ± 0.02^{g}	5.10 ± 0.02^{e}	6.18 ± 0.02^{e}
20	460.5 ± 0.9^{f}	162.3 ± 0.5^{f}	81.5 ± 0.4^{f}	72.3 ± 0.4^{f}	15.54 ± 0.04^{f}	12.02 ± 0.01^{d}	14.27 ± 0.03^{d}
22	1334.9 ± 1.1^{e}	246.1 ± 0.4^{e}	153.1 ± 0.4^{e}	128.7 ± 0.5^{e}	24.47 ± 0.05^{e}	16.18 ± 0.03^{c}	17.25 ± 0.05^{c}
24	2001.2 ± 1.3^{d}	349.4 ± 0.5^{d}	226.6 ± 0.9^{d}	245.5 ± 0.6^{d}	32.01 ± 0.06^{d}	17.37 ± 0.04^{b}	18.12 ± 0.06^{b}
26	2158.9 ± 1.2^{c}	369.5 ± 0.7^{c}	254.5 ± 0.8^{c}	268.4 ± 0.7^{c}	33.14 ± 0.07^{c}	17.55 ± 0.05^{a}	18.33 ± 0.07^{a}
28	2198.2 ± 1.2^{b}	372.1 ± 0.9^{b}	256.3 ± 0.6^{b}	272.4 ± 0.9^{b}	33.32 ± 0.09^{b}	17.40 ± 0.06^{b}	18.42 ± 0.10^{a}
30	2280.3 ± 1.3^{a}	388.8 ± 0.9^{a}	259.4 ± 0.7^{a}	281.6 ± 0.8^{a}	33.69 ± 0.10^{a}	17.49 ± 0.07^{ab}	18.36 ± 0.09^{a}

Values are expressed as mean ± standard error (Mean ± SE), and values marked with no identical letters in the same column indicate significant differences ($P < 0.05$, $n = 6$).
Abbreviation: E, embryonic age.

at E22 to E24, with an average daily increment of 51.6 mg/each. When comparing E18 to E22, feather mass increased more slowly compared to E22 to E24, with an average daily gain of 46.2 mg/head. and from E24 to E30, the back of the embryo was more mature and feather mass could reach 388.8 mg/head on average at E30.

As shown in Table 4 and compared to the Gompertz and von Bertalanffy models, the logistic model had the largest fit ($R^2 = 0.997$) and the smallest sum of squares of residuals (RSS = 611.83), Akaike's information criterion (AIC = 43.973), Bayesian information criterion (BIC = 44.565), and mean squared error (MSE = 67.981) were minimal. The inflection point for back feather growth was E20.7, the inflection point feather mass was 193.5 mg, and the maximum daily gain was 56.1 mg. As shown in Figure 4a, the predicted values from the logistic model were closer to the measured values of the back feather mass of the goose embryos. Therefore, the logistic model is more suitable for describing the changes in back feather growth during the embryonic period of the Jilin white goose.

Variation pattern of goose embryo chest feather mass and model fitting analysis

As can be seen from Table 3, the embryonic chest feathers of Jilin white geese (*A. cygnoides*) start to grow from E14, and the feather mass grows slowly from E14 to E18. The period of rapid growth lasts from E18 to E24, and the feather mass increases at the quickest rate from E22 to E24, with an average daily gain of 36.8 mg/each; Compared to E22 to E24, feather mass increased at a slower rate from E18 to E22, with an average daily gain of 33.7 mg per bird. Moreover, the goose embryo had more mature feather development at E24 to E30 and could reach an average feather mass of 259.4 mg per bird at E30.

As shown in Table 4, compared to the Gompertz and von Bertalanffy models, the logistic model had the largest fit ($R^2 = 0.999$) and the lowest sum of residual squares (RSS = 149.91), Akaike's information criterion (AIC = 31.315), Bayesian information criterion (BIC = 31.907), and mean squared error (MSE = 16.657), which were minimal. The inflection point for chest feather growth was E21.5, with an inflection point feather mass of 130.6 mg and a maximum daily gain of 44.4 mg. As shown in Figure 4b, the predicted values from the logistic model were closer to the measured values of chest feather mass in goose embryos. Therefore, the logistic model is more suitable for describing the changes in chest feather growth during the embryonic period of the Jilin white goose.

Model fit analysis and variation pattern of goose embryo belly feather mass

As can be seen from Table 3, the embryonic belly feathers of the Jilin white goose start to grow from E14, and the feather mass grows slowly from E14 to E18; The period of rapid growth lasts from E18 to E24, and the feather mass increases at the quickest rate from E22 to E24, with an average daily gain of 58.4 mg/each. In contrast, the feather mass grows at a slower rate from E18 to E22, compared to the E22 to E24 stage, with an average daily gain of 27.9 mg/each. However, from E24 to E30, the goose embryos had more mature belly feather development and could reach an average feather mass of 281.6 mg/head at E30.

As shown in Table 4, compared to the Gompertz and von Bertalanffy models, the logistic model had the highest fit ($R^2 = 0.994$) and sum of residual squares (RSS = 770.56), Akaike's information criterion (AIC = 46.049), Bayesian information criterion (BIC = 46.641), and mean squared error (MSE = 85.618) were minimal. The inflection point for belly feather growth was E21.9, the inflection point feather mass was 141.4 mg and the maximum daily increment was 49.5 mg. As shown in Figure 4c, the predicted values from the logistic model were closer to the measured values of the belly feather mass of goose embryos. Therefore, the logistic model is more suitable for describing the changes in belly feather growth during the embryonic period of the Jilin white goose.

Back feather length variation pattern in goose embryos and model fitting analysis

From Table 3, it can be seen that the length of the back feathers of the Jilin white goose during the embryonic period increased with the increase of embryonic age. Among them, the E20 to E22 back feather length grew the fastest with an average daily increment of 4.47 mm/root, the E22 to E24 feather length grew faster with an average daily increment of

Table 4. Fitted curve model and parameters for embryonic feather mass in Jilin white goose

Site	Growth model	Expressions[1]	Inflectionfeather mass (mg)	Inflection day (E)	Maximum daily gain (mg)	R^2	RSS	AIC	BIC	MSE
Whole body	Logistic	$Y = 2253.12/(1 + 15087181.35e^{-0.77t})$	1126.6	21.5	433.7	0.997	25661.67	77.600	78.191	2851.296
	Gompertz	$Y = 2295.61e^{-64027.86exp(-0.53t)}$	1147.8	20.9	304.2	0.991	70389.05	86.681	87.273	7821.005
	von Bertalanffy	$Y = 2682.81(1–31.97e^{-0.23t})^3$	1341.4	15.1	154.3	0.971	229264.26	97.309	97.900	25473.807
Back	Logistic	$Y = 386.91/(1 + 163246.56e^{-0.58t})$	193.5	20.7	56.1	0.997	611.83	43.973	44.565	67.981
	Gompertz	$Y = 400.65e^{-1474.71exp(-0.37t)}$	200.3	19.7	37.1	0.994	1213.32	50.135	50.727	134.814
	von Bertalanffy	$Y = 424.14(1–47.50e^{-0.26t})^3$	212.1	14.8	27.6	0.989	2243.17	55.666	56.257	249.241
Chest	Logistic	$Y = 261.25/(1 + 2249370.92e^{-0.68t})$	130.6	21.5	44.4	0.999	149.91	31.315	31.907	16.657
	Gompertz	$Y = 268.67e^{-8465.32exp(-0.44t)}$	134.3	20.6	29.6	0.997	296.60	37.456	38.048	32.956
	von Bertalanffy	$Y = 301.69(1–38.16e^{-0.24t})^3$	150.8	15.2	18.1	0.984	1711.00	53.228	53.820	190.111
Belly	Logistic	$Y = 282.80/(1 + 4659215.43e^{-0.70t})$	141.4	21.9	49.5	0.994	770.56	46.049	46.641	85.618
	Gompertz	$Y = 293.04e^{-8478.03exp(-0.43t)}$	146.5	21.0	31.5	0.988	1429.96	51.614	52.205	158.884
	von Bertalanffy	$Y = 340.72(1–27.68e^{-0.22t})^3$	170.4	15.1	18.7	0.973	3333.68	59.231	59.823	370.409

Abbreviations: AIC, Akaike's information criterion; BIC, Bayesian information criterion; E, embryonic age; MSE, mean square error. R^2, R-squared. RSS, residual sum of squares.
[1] *Y* is the mass of the goose embryo feathers observed at *t* embryonic age; *t* is the embryonic age; *e* is a natural constant; exp is the mathematical symbol.

3.77 mm/root and the E24 to E30 feather length grew slower and reached an average of 33.69 mm/root at E30.

From the fitted curve model of back feather length at the embryonic stage of the Jilin white goose in Table 5, it can be seen that the logistic model had the largest fit (R^2 = 0.982) and the smallest residual sum of squares (RSS = 20.34), Akaike's information criterion (AIC = 13.340), Bayesian information criterion (BIC = 13.931), and mean square error (MSE = 2.260). The inflection point embryonic age for back feather growth was E20.1, the inflection point feather length was 17.7 mm and the maximum daily increment was 3.4 mm. As seen in Figure 4d, the measured values of back feather length were close to the predicted values of the Logistic curve compared to the Gompertz and von Bertalanffy curves. Therefore, the logistic model was better at describing the variation in back feather length during the embryonic period in Jilin white geese.

Model fitting analysis and variation pattern of chest feather length in goose embryos

From Table 3, it can be seen that the length of the chest feathers of the Jilin white goose during the embryonic period increased with the increase of embryonic age. Among them, the E18 to E20 chest feather length grew the fastest, with an average daily increment of 3.46 mm/root, following, the E20 to E22 feather length grew faster, with an average daily increment of 2.08 mm/root and the E22 to E30 feather length grew slower and reached an average of 17.49 mm/root at E30.

From the fitted curve model of the chest feather length during the embryonic period of the Jilin white goose in Table 5, it can be seen that the logistic model had the largest fit (R^2 = 0.998) and the smallest residual sum of squares (RSS = 0.82), Akaike's information criterion (AIC = −15.517), Bayesian information criterion (BIC = −14.926), and mean square error (MSE = 0.092). In particular, the inflection point embryonic age for thoracic feather growth was E19.1, the inflection point feather length was 8.8 mm and the maximum daily increment was 3.3 mm. As shown in Figure 4e, the measured values of thoracic feather length compared to the Gompertz and von Bertalanffy curves largely matched the predicted values of the Logistic curve. Therefore, the changes in chest feather length during the embryonic period of Jilin white geese (*A. cygnoides*) were best characterized by the logistic model.

Model fitting analysis and variation pattern of belly feather length in goose embryos

Table 3 shows that the length of the Jilin white goose's belly feathers during the embryonic stage increased as the embryonic age increased. E18 to E20 belly feather length increased the fastest, averaging 4.05 mm/root per day, followed by E14 to E18 feather length, which increased by 1.4 mm/root per day, and E22 to E30 feather length, which increased more slowly, averaging 18.36 mm/root per day at E30. From the fitted curve model of the belly feather length during the embryonic period of the Jilin white goose in Table 5, it can be seen that the logistic model had the largest fit (R^2 = 0.998) and the smallest residual sum of squares (RSS = 1.09), Akaike's information criterion (AIC = −12.975), Bayesian information criterion (BIC = −12.383), and mean square error (MSE = 0.121). The inflection point for belly feather growth was E18.7, with an inflection point feather length of 9.2 mm and a maximum daily increment of 3.8 mm. As can be seen from Figure 4f, the

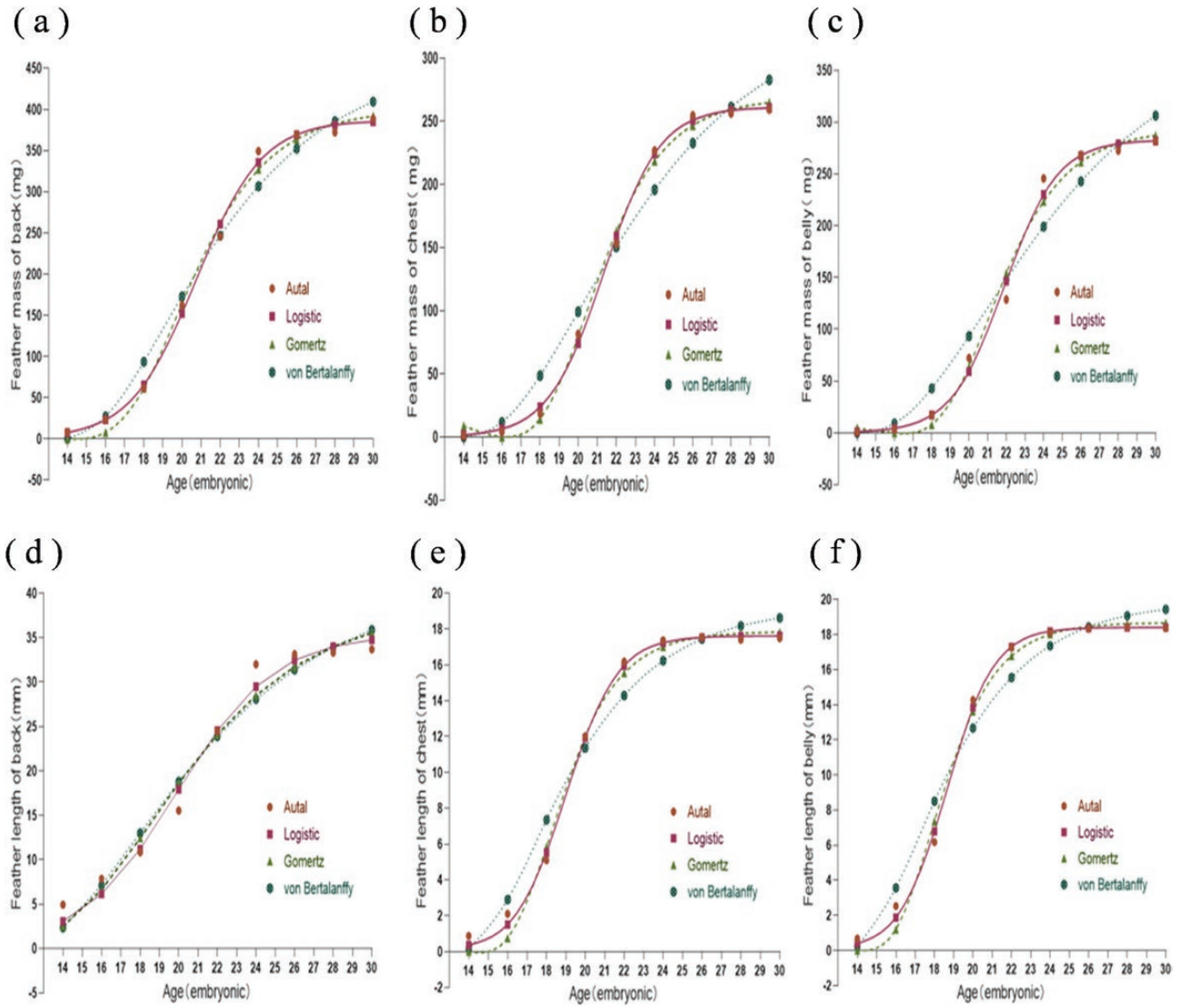

Figure 4. Actual measurements of feather mass and feather length at different parts of the embryonic stage of the Jilin white goose were fitted to predicted values from three growth models, Logistic, Gompertz, and Von Bertalanffy. (a) Feather mass on the back. (b) Feather mass on the chest. (c) Feather mass on the belly. (d) The length of the feathers on the back. (e) Feather length on the chest. (f) Feather length on the belly.

measured values of belly feather length were mostly distributed on the logistic curve compared to the Gompertz and von Bertalanffy curves. Therefore, the logistic model was more accurate in describing the variation in belly feather length during the embryonic period in Jilin white geese.

Discussion

The process of feather follicle development

Feather follicles are the basis for the growth and development of poultry feathers, which are gathered into different feather bundles, and their occurrence is influenced by a combination of epithelial and mesenchymal cells (Wang et al., 2017). In the present study, the epidermis was found to begin to bulge at E12, marking the formation of feather buds, whereas in chicken embryos the epidermis began to form feather buds at E9 (Widelitz et al., 2003), probably because the embryonic development period is longer in geese than in chickens, and presumably the feather follicles developed and formed later in goose embryos than in chicken embryos. The results of this study showed that feather follicles of the goose embryo were formed from E12 to E20, and that follicle morphogenesis was almost complete at E20, which is consistent with the chicken embryo follicle development stages E9 to E15. In addition, goose embryo forms primary feather follicles at approximately E14 and secondary feather follicles at E18 (Figure 1B). Studies on the morphogenesis of feather follicles during the embryonic period of the Carlos goose have shown that primary feather follicles are formed at E13 and secondary feather follicles at E18 in goose embryos (Liu et al., 2018), while in studies on the development of feather follicles during the embryonic period of the breeding goose, E9 was found to be the early stage of dermal agglutination, E13 the short bud period, and E17 the long bud period (Feng et al., 2022), which is consistent with the process of feather follicle formation of the Jilin white goose in this experiment. In the meantime, to better characterize the development of feather follicles in different regions of poultry, feather follicles are generally divided into primary and secondary follicles. The study has shown that primary and secondary follicles develop independently

Table 5. Fitted curve model and feather length parameters in Jilin white goose embryos

Site	Growth model	Expressions	Inflection feather length (mm)	Inflection day (E)	Maximum daily gain (mm)	R^2	RSS	AIC	BIC	MSE
Back	Logistic	$Y = 35.61/(1 + 2082.31e^{-0.38t})$	17.8	20.1	3.4	0.982	20.34	13.340	13.931	2.260
	Gompertz	$Y = 38.63e^{-57.46exp(-0.22t)}$	19.3	18.4	2.1	0.967	37.64	18.878	19.469	4.182
	von Bertalanffy	$Y = 41.19(1-6.04e^{-0.16t})^3$	20.6	11.2	1.6	0.960	46.18	20.718	21.310	5.131
Chest	Logistic	$Y = 17.62/(1 + 1991477.89e^{-0.76t})$	8.8	19.1	3.3	0.998	0.82	−15.517	−14.926	0.092
	Gompertz	$Y = 17.86e^{-13359.54exp(-0.52t)}$	8.9	18.3	2.3	0.990	3.92	−1.473	−0.882	0.436
	von Bertalanffy	$Y = 18.37(1-195.61e^{-0.36t})^3$	9.2	14.7	1.7	0.982	7.33	4.150	4.742	0.814
Belly	Logistic	$Y = 18.41/(1 + 4542680.23e^{-0.82t})$	9.2	18.7	3.8	0.998	1.09	−12.975	−12.383	0.121
	Gompertz	$Y = 18.69e^{-15608.29exp(-0.54t)}$	9.3	17.9	2.5	0.990	4.41	−0.428	0.163	0.490
	von Bertalanffy	$Y = 19.07(1-303.78e^{-0.39t})^3$	9.5	14.7	1.9	0.983	7.42	4.263	4.854	0.824

Abbreviations: AIC, Akaike's information criterion; BIC, Bayesian information criterion; E, embryonic age; MSE, mean square error. R^2, R-squared. RSS, residual sum of squares.
[1] Y is the length of the goose embryo feathers observed at *t* embryonic age; *t* is the embryonic age; *e* is a natural constant; exp is the mathematical symbol.

and both originate from the feather primordium and the developing of primary follicles is earlier than secondary follicles (Xu et al., 2007). In a study of embryonic skin follicles in yellow-feathered broiler chickens, the authors found that primary feather follicles began to form at E12. By E15, primary feather follicles matured and secondary feather follicles emerged, both developing independently, with the formation of primary feather follicles preceding secondary feather follicles (Xie et al., 2020a). However, some studies have found that secondary hair follicles in sheep develop from primary hair follicles, but the reason for the difference between the two needs to be further investigated (Ferguson et al., 2012).

Microstructure and density of feather follicles

In this study, histological observations of feather follicles in goose embryos showed that the first feather branchial ridges in the follicle structure appeared at E14 and that each feather branchial ridge could be differentiated into a marginal plate, a feather branchlet plate, and a feather axial plate. A similar finding was reported by Xu et al. (2007).

At the same time, a previous study found that the dermal cell condensation in geese occurs at E9, which is thought to be the beginning of hair follicle development, and the primary feather follicles begin to form at E13 (Feng et al., 2022). At this stage, blood vessels begin to appear in the central zone of the dentary, which is composed of fibroblasts and an extracellular matrix (Yu et al., 2004). During the development of feather follicles, their density plays a crucial role in feather production and quality. In this study, it was found that the primary feather follicles of goose embryos began to appear at E14, and their density generally showed a trend of first increasing and then decreasing, reaching the maximum density at the emergence of secondary feather follicles at E18; while the density of secondary feather follicles gradually increased from E18 until they emerged from the shell, which was basically consistent with the results of Chen et al. (2012), indicating that feather follicle development nodes of Jilin White Goose and Wanxi White Goose were similar. However, it was found that the secondary feather follicle development period of Jilin White Goose was E18, whereas that of Wanxi White Goose was close to E20, concluding that the secondary feather follicle formation period of Wanxi White Goose was slightly later than that of Jilin White Goose, which might be caused by factors such as geography, climate, and breed differences (Scott et al., 2015).

Goose embryo feather growth and development patterns

Feather follicle development is one of the important growth aspects during embryogenesis in birds (Chen et al., 2015; Ng et al., 2018). For geese, particularly the development of feather follicles, largely determines feather length and weight, which in turn affects feather-related economic traits (Lu et al., 2015). Therefore, by modeling growth curves, we can dynamically describe and profile the growth process between feather mass and length and embryonic age in Jilin white geese (*A. cygnoides*) during the embryonic period. Currently, studies have been conducted on the growth of thoracic and belly feathers in yellow-finned broilers, but modeling growth curves for whole-body feather mass and the weight and length of back, thoracic, and belly feathers in goose embryos have not been reported (Xie et al., 2020b).

In this study, we found that a logistic curve model fitted best to the embryonic feather growth and development of Jilin white geese. Feathers started to grow slowly from E14 to E18, showed rapid growth from E18 to E24, and after E24, the feather growth rate decreased until just before emergence (E30). This result shows the different intensities of different growth stages in the feather formation process. In addition, we found that the logistic curve model was more suitable for describing the changes in feather growth during the embryonic stage of Jilin white geese, but this result is inconsistent with the study of feather growth in yellow-feathered broilers by Xie et al. (2020b), probably because chickens are not important down-producing animals and their own feathers only provide insulation and body protection, whereas goose feathers can also be used as an important textile material (Xie et al., 2020b).

In this study, we found that before E14, embryonic feathers were concentrated in the back region and no feathers were found on the head, neck, chest, abdomen, or wings. By E22, the whole body of the embryo was covered with feathers, and back feathers were the earliest and fastest to develop, which is basically consistent with the change in feather growth of chicken embryos (Meyer and Baumgartner 1998). Meanwhile, we found that the inflection point of feather mass in goose embryos was around E21, while feather length occurred at E19. Although Xie et al. (2020b) showed that the inflection points of feather mass and length in yellow-finned broiler embryos were at E14 and E12, E11 to E15 was the fastest feather growth stage. Moreover, a study by Meyer and Baumgartner (1998) showed that the fastest feather growth rate in the embryonic stage of the white Lai hang chickens was E14 to E15. It can be assumed that goose and chicken embryos reach the inflection point of feather length in preference to feather mass. In addition, studies have shown that E12 to E14 for chicken embryos and E19 to E21 for goose embryos, are the periods of secondary follicle development during which the primary follicle density reaches its highest stage, so the growth inflection points of feather length and feather mass may be influenced by the growth and development of primary and secondary follicles.

Conclusions

In summary, the primary follicle development time of the Jilin white goose was E14 and the secondary follicle development time was E18. The primary follicle density showed a trend of first increasing and then decreasing, whereas the secondary follicle density showed a continuously increasing trend and the primary and secondary follicles developed independently. Furthermore, the logistic curve model better fits the embryonic feather growth and development of Jilin white geese. At the same time, using the growth curve model to explain the relationship between feather growth and embryonic age in geese will potentially speed up the process of genetic improvement in Jilin white geese (*A. cygnoides*) and thus provide scientific support for molecular genetic breeding. Of course, this approach needs to be revalidated in subsequent studies.

Supplementary Data

Supplementary data are available at *Journal of Animal Science* online.

Acknowledgments

This work was supported by the Department of Science and Technology of Jilin Province, the Young and Middle-aged Science and Technology Innovation Leaders and Teams, and the Jilin Province Goose Germplasm Resources and Genetic Improvement Innovation Team (20200301035RQ), the Development and Utilization Project of Livestock and Poultry Genetic Resources, and the Breeding and Extension Demonstration of Carlos Goose and Jilin White Goose Mating Lines (2022).

Conflict of Interest

The authors confirm that they have no conflict of interest.

References

Aggrey, S. E. 2002. Comparison of three nonlinear and spline regression models for describing chicken growth curves. *Poult. Sci.* 81:1782–1788. doi:10.1093/ps/81.12.1782

Boz, M. A., F. Oz, U. S. Yamak, M. Sarica, and E. Cilavdaroglu. 2019. The carcass traits, carcass nutrient composition, amino acid, fatty acid, and cholesterol contents of local Turkish goose varieties reared in an extensive production system. *Poult. Sci.* 98:3067–3080. doi:10.3382/ps/pez125

Chen, X., H. Bai, L. Li, W. Zhang, R. Jiang, and Z. Geng. 2012. Follicle characteristics and follicle developmental related Wnt6 polymorphism in Chinese indigenous Wanxi-white goose. *Mol. Biol. Rep.* 39:9843–9848. doi:10.1007/s11033-012-1850-2

Chen, C. F., J. Foley, P. C. Tang, A. Li, T. X. Jiang, P. Wu, R. B. Widelitz, and C. M. Chuong. 2015. Development, regeneration, and evolution of feathers. *Annu. Rev. Anim. Biosci.* 3:169–195. doi:10.1146/annurev-animal-022513-114127.

Chen, C. C., M. V. Plikus, P. C. Tang, R. B. Widelitz, and C. M. Chuong. 2016. The modulatable stem cell niche: tissue interactions during hair and feather follicle regeneration. *J. Mol. Biol.* 428:1423–1440. doi:10.1016/j.jmb.2015.07.009

Feng, Z., H. Gong, J. Fu, X. Xu, Y. Song, X. Yan, I. Mabrouk, Y. Zhou, Y. Wang, X. Fu, et al. 2022. *In Ovo* injection of CHIR-99021 promotes feather follicle development *via* modulating the wnt signaling pathway and transcriptome in goose embryos (*Anser cygnoides*). *Front. Physiol.* 13:858274. doi:10.1016/j.psj.2022.101825

Ferguson M. B., B. A. McGregor, R. Behrendt. 2012. Relationships between skin follicle characteristics and fibre properties of Suri and Huacaya alpacas and Peppin Merino sheep. *Anim. Prod. Sci.* 52:442–447. doi:10.1071/an11233

Gao, C. Q., J. X. Yang, M. X. Chen, H. C. Yan, and X. Q. Wang. 2016 Apr. Growth curves and age-related changes in carcass characteristics, organs, serum parameters, and intestinal transporter gene expression in domestic pigeon (*Columba livia*). *Poult. Sci.* 95:867–877. doi:10.3382/ps/pev443

Guo, B. B., Z. C. Dai, Y. H. Ren, H. X. Zhu, X. B. Shao, A. D. Sun, and Z. D. Shi. 2021. Improvement of goose embryonic and muscular developments by wider angle egg turning during incubation and the regulatory mechanisms. *Poult. Sci.* 100:101477. doi:10.1016/j.psj.2021.101477

Hu, X. W., X. K. Zhang, Z. W. Liu, et al. 2020. Exploration of key regulators driving primary feather follicle induction in goose skin. *Gene*. 731:144338. doi:10.1016/j.gene.2020.144338

Kondo, M., Sekine, T., Miyakoshi, T., Kitajima, K., Egawa, S., Seki, R., … Tamura K. 2018. Flight feather development: its early specialization during embryogenesis. *Zool. Lett.*, 4(1). doi:10.1186/s40851-017-0085-4

Kozák, J., I. Gara, and T. Kawada. 2010. Production and welfare aspects of goose down and feather harvesting. *World Poul.Sci. J.* 66:767–778. doi:10.1017/s0043933910000723

Liu, C., C. T. Sello, Y. Sun, Y. Zhou, H. Lu, Y. Sui, J. Hu, C. Xu, Y. Sun, J. Liu, et al. 2018. *De Novo* transcriptome sequencing analysis of goose (*Anser anser*) embryonic skin and the identification of genes related to feather follicle morphogenesis at three stages of development. *Int. J. Mol. Sci.* 19:3170. doi:10.3390/ijms19103170

Lu, L., Y. Chen, Z. Wang, X. Li, W. Chen, Z. Tao, and J. Wang. 2015. The goose genome sequence leads to insights into the evolution of waterfowl and susceptibility to fatty liver. *Genome Biol.* 16. doi:10.1186/s13059-015-0652-y

Mabrouk, I., Y. Zhou, S. Wang, Y. Song, X. Fu, X. Xu, T. Liu, Y. Wang, Z. Feng, J. Fu, et al. 2022. Transcriptional characteristics showed that miR-144-y/FOXO3 participates in embryonic skin and feather follicle development in zhedong white goose. *Animals (Basel)* 12:2099. doi:10.3390/ani12162099

Martel JL, Miao JH, Badri T, 2022. Anatomy, hair follicle. 2021 Oct 14. In: *StatPearls [Internet]*. Treasure Island (FL): StatPearls Publishing; Jan–. PMID: 29261946.

Meyer, W., and G. Baumgartner. 1998. Embryonal feather growth in the chicken. *J. Anat.* 193:611–616. doi:10.1046/j.1469-7580.1998.19340611.x

Narinc, D., E. Karaman, T. Aksoy, and M. Z. Firat. 2013. Investigation of nonlinear models to describe long-term egg production in Japanese quail. *Poult. Sci.* 92:1676–1682. doi:10.3382/ps.2012-02511

Ng, C. S., and W. H. Li. 2018. Genetic and molecular basis of feather diversity in birds. *Genome Biol. Evol.* 10:2572–2586. doi:10.1093/gbe/evy180

Nguyen, T. H., C. X. Nguyen, M. Q. Luu, A. T. Nguyen, D. H. Bui, D. K. Pham, and D. N. Do. 2021. Do DN. Mathematical models to describe the growth curves of Vietnamese Ri chicken. *Braz. J. Biol.* 83:e249756. doi:10.1590/1519-6984.249756

Ricklefs, R. E. 1985. Modification of growth and development of muscles of poultry[J]. *Poult. Sci.* 64:1563–1576. doi:10.3382/ps.0641563

Scott, J. M., J. D. Costa, and E. O. Oviedorondon. 2015. Incubation temperature profiles affect broiler feathering. *J. Appl. Poult. Res.* 24:49–57. doi:10.3382/japr/pfu022

Tompic, T., J. Dobsa, S. Legen, N. Tompic, and H. Medic. 2011. Modeling the growth pattern of in-season and off-season Ross 308 broiler breeder flocks. *Poult. Sci.* 90:2879–2887. doi:10.3382/ps.2010-01301

Vitezica, Z. G., C. Marie-Etancelin, M. D. Bernadet, X. Fernandez, and C. Robert-Granie. 2010. Comparison of nonlinear and spline regression models for describing mule duck growth curves. *Poult. Sci.* 89:1778–1784. doi:10.3382/ps.2009-00581

Wang, A. B., Y. V. Zhang, and T. Tumbar. 2017. Gata6 promotes hair follicle progenitor cell renewal by genome maintenance during proliferation. *EMBO J.* 36:61–78. doi:10.15252/embj.201694572

Widelitz, R. B., T. X. Jiang, M. K. Yu, T. Shen, J. Y. Shen, P. Wu, Z. Yu, and C. M. Chuong. 2003. Molecular biology of feather morphogenesis: A testable model for evo-devo research. *J. Exp. Zool.* 298B:109–122. doi:10.1002/jez.b.29

Wu, W., R. F. Xu, X. Guo, C. H. Li, and C. X. Wu. 2008. Characterization of embryonic feather follicle development in the Chinese indigenous Jilin white goose. *Asian Australas. J. Anim.* 21:346–352. doi:10.5713/ajas.2008.70302

Xie, W. Y., M. J. Chen, S. G. Jiang, H. C. Yan, X. Q. Wang, and C. Q. Gao. 2020a. Investigation of feather follicle morphogenesis and the expression of the Wnt/β-catenin signaling pathway in yellow feathered broiler chick embryos. *Br. Poult. Sci*, 61:5, 557–565. doi:10.1080/00071668.2020.1758302

Xie, W. Y., N. X. Pan, H. R. Zeng, H. C. Yan, X. Q. Wang, and C. Q. Gao. 2020b. Comparison of nonlinear models to describe the feather growth and development curve in yellow-feathered chickens. *Animal.* 14:1005–1013. doi:10.1017/S1751731119003082

Xu, R. F., W. Wu, and H. Xu. 2007. Investigation of feather follicle development in embryonic geese[J]. *Poult. Sci.* 86:2000–2007. doi:10.1093/ps/86.9.2000

Yu, M., Z. Yue, P. Wu, D. Y. Wu, J. A. Mayer, M. Medina, R. B. Widelitz, T. X. Jiang, and C. M. Chuong. 2004. The biology of feather follicles. *Int. J. Dev. Biol.* 48:181–191. doi:10.1387/ijdb.031776my

Zou, M., L. Xu, J. Zhou, J. Song, S. Liu, and X. Li. 2020. Microstructure and compression resistance of bean goose (*Anser fabalis*) feather shaft. *Microsc. Res. Tech.* 83:156–164. doi:10.1002/jemt.23398